

Unconstrained parameter estimation for assessment of dynamic cerebral autoregulation

This content has been downloaded from IOPscience. Please scroll down to see the full text.

2008 Physiol. Meas. 29 1179

(<http://iopscience.iop.org/0967-3334/29/10/003>)

View [the table of contents for this issue](#), or go to the [journal homepage](#) for more

Download details:

IP Address: 128.111.121.42

This content was downloaded on 07/09/2015 at 07:59

Please note that [terms and conditions apply](#).

Unconstrained parameter estimation for assessment of dynamic cerebral autoregulation

M Chacón¹, N Nuñez¹, C Henríquez¹ and R B Panerai^{2,3}

¹ Departamento de Ingeniería Informática, Universidad de Santiago de Chile, Santiago, Chile

² Department of Cardiovascular Sciences, University of Leicester, Leicester, UK

E-mail: rp9@le.ac.uk

Received 16 April 2008, accepted for publication 25 July 2008

Published 17 September 2008

Online at stacks.iop.org/PM/29/1179

Abstract

Measurement of dynamic cerebral autoregulation (CA), the transient response of cerebral blood flow (CBF) to changes in arterial blood pressure (ABP), has been performed with an index of autoregulation (ARI), related to the parameters of a second-order differential equation model, namely gain (K), damping factor (D) and time constant (T). Limitations of the ARI were addressed by increasing its numerical resolution and generalizing the parameter space. In 16 healthy subjects, recordings of ABP (Finapres) and CBF velocity (ultrasound Doppler) were performed at rest, before, during and after 5% CO₂ breathing, and for six repeated thigh cuff maneuvers. The unconstrained model produced lower predictive error ($p < 0.001$) than the original model. Unconstrained parameters ($K'-D'-T'$) were significantly different from $K-D-T$ but were still sensitive to different measurement conditions, such as the under-regulation induced by hypercapnia. The intra-subject variability of K' was significantly lower than that of the ARI and this parameter did not show the unexpected occurrences of zero values as observed with the ARI and the classical value of K . These results suggest that K' could be considered as a more stable and reliable index of dynamic autoregulation than ARI. Further studies are needed to validate this new index under different clinical conditions.

Keywords: cerebral blood flow, arterial blood pressure, cerebral haemodynamics, dynamic cerebral autoregulation index

1. Introduction

Transcranial Doppler ultrasound (TCD) allows continuous recordings of cerebral blood flow velocity (CBFV) with high temporal resolution, but the interpretation and clinical application

³ Corresponding address: Department of Medical Physics, Leicester Royal Infirmary, Leicester LE1 5WW, UK.

of CBFV measurements are not straightforward. Although TCD does not provide a direct measure of absolute cerebral blood flow (CBF), CBFV can be assumed to reflect changes in CBF, as long as the diameter of the insonated vessel remains constant. The main difficulty with the interpretation of CBFV recordings though is the complexity of the regulatory mechanisms that control CBF maintaining its value within narrow limits, to match oxygen supply and demand, and to protect the brain against perturbations in arterial blood pressure (ABP). The ability to model and quantify the influence of ABP and several other variables on CBF/CBFV is an important requisite to improve the clinical usefulness of TCD.

The demonstration by Aaslid *et al* (1989) that cerebral autoregulation can be described as a dynamic phenomenon led to a surge of research in this area and stimulated the search for analytical methods to extract clinically relevant information from physiological measurements. The classical definition of cerebral autoregulation, as the ability of the cerebral circulation to maintain cerebral blood flow (CBF) relatively constant, despite large changes in arterial blood pressure (ABP) in the range of 60–150 mmHg (Paulson *et al* 1990), is now regarded as the ‘static’ approach since in most studies measurements of ABP and CBF were averaged over several minutes. The excellent temporal resolution of TCD has allowed Aaslid *et al* (1989) to record the transient changes in CBF velocity (CBFV) that accompany a sudden change in ABP, which is the essence of the concept of *dynamic* cerebral autoregulation (dCA).

Initial attempts to quantify dCA were based in the rate of change of the CBFV response (Aaslid *et al* 1989, Steiger *et al* 1994), but, in 1995, Tiecks *et al* introduced the autoregulation index (ARI), based on ten possible ‘template’ CBFV responses to an idealized step change in ABP. A value of the ARI was assigned to each of these template curves, varying from $ARI = 0$, for the absence of autoregulation, to a maximum of $ARI = 9$, to represent the most efficient autoregulatory responses that can be observed. The simplicity of this approach, and its availability at the push of a button, in at least one commercial TCD machine, has led to its widespread use in physiological and clinical studies of dCA. The examples include the effects of aging (Carey *et al* 2000), adolescence (Vavilala *et al* 2002), temperature (Doering *et al* 1999) and breathing rate (Panerai *et al* 2003) on dCA. Some of the clinical conditions assessed were severe head injury (Junger *et al* 1997), stroke (Dawson *et al* 2000), carotid artery disease (White and Markus 1997), carotid sinus syndrome (Leftheriotis *et al* 2000) and hypertension (Eames *et al* 2003).

The ARI was initially proposed to quantify CBFV responses induced by the thigh cuff maneuver (Tiecks *et al* 1995). Almost simultaneously, it became apparent that dCA could also be assessed from spontaneous fluctuations of ABP and CBFV (Giller 1990, Panerai *et al* 1995, Steinmeier *et al* 1996), and it was later demonstrated that the values of ARI could also be extracted from spontaneous fluctuations (Panerai *et al* 1999a, 2001). This finding is of some importance, since it allows the extraction of clinically relevant information without the risk, or inconvenience, of disturbing ABP in critically ill patients. However, when using the ARI in conjunction with spontaneous fluctuations of ABP and CBFV, a number of limitations in this method became apparent, some of which also apply to its derivation from thigh cuff maneuvers. First of all, a very high variability was observed, including the possibility of values of $ARI = 0$ in healthy subjects (Mahony *et al* 2000, Panerai *et al* 2003, Simpson *et al* 2004). This high variability is likely to limit the reproducibility of assessments and the usefulness of the ARI for clinical applications involving single individuals, rather than groups of patients (Panerai *et al* 2004). In repeated thigh cuff maneuvers, Mahony *et al* (2000) also reported an intra-subject variability of 37% in the ARI. The second major limitation of the ARI is the use of fixed combinations of the three basic parameters that describe the temporal pattern of the ten template CBFV response curves, namely the gain (K), time constant (T) and damping ratio (D) of the second-order differential equation model proposed by Tiecks

et al (1995). Theoretically, it is possible that other combinations of K , D , T could lead to a much better fitting of CBFV transient responses than those allowed by the ten combinations of these parameters, corresponding to the associated values of the ARI. If this is true, it is also possible that these alternative combinations of K , D , T could lead to more stable and reproducible results than afforded by the classical calculation of the ARI. Finally, the discrete nature of the ARI scale is also undesirable. If the number of possible states could be significantly increased, there could be a reduction in the variability of the ARI, as expressed by the standard deviation of differences.

To address the limitations of the ARI mentioned above, we analyzed a database of recordings from healthy subjects, containing both spontaneous fluctuations in ABP and CBFV, as well as repeated thigh cuff maneuvers. We tested the hypothesis that allowing the parameter set (K , D , T) to assume a wider range of values would lead to improved fitting of CBFV transient responses and would also reduce the variability of the ARI. This study is an essential first step in the direction of finding a more general and potentially more reproducible index of dynamic cerebral autoregulation.

2. Methods

2.1. Subjects and measurements

A database of recordings from 16 healthy subjects (mean \pm SD age: 30 ± 7 years old) provided the data for this study. As described previously (Panerai *et al* 1999b, Mahony *et al* 2000), measurements were performed at rest, in the supine position, during six repeated thigh cuff maneuvers and also included a CO₂ reactivity test. The study was approved by the local ethic committee and written informed consent was obtained from each subject. Measurements were performed in a temperature-controlled laboratory.

CBFV was recorded from the right middle cerebral artery (MCA), with a SciMed QVL-120 transcranial Doppler ultrasound device and a 2 MHz transducer. The depth of insonation varied between 45 and 50 mm. ABP was measured continuously with a non-invasive pressure monitor (Finapres 2300, Ohmeda, Colorado, USA). End-tidal CO₂ (EtCO₂) was measured with an infrared capnograph (Datex Normocap 200) connected to a closely fitting face mask at rest, but not during thigh cuff maneuvers. A three-lead ECG was also continuously recorded. When all measurements were stable for at least 15 min, a calibration signal from the Finapres was recorded, the servo-system was switched off and recordings were made on a digital audio tape (Sony PC108M). For the thigh cuff maneuvers, appropriately sized cuffs were inflated above systolic ABP for at least 3 min on both thighs. Recordings started during the inflation phase and continued for at least 3 min after the cuffs were rapidly deflated. A total of six maneuvers were performed for each subject. Between each maneuver the servo-control of the Finapres was switched back on, the subjects were allowed to rest for at least 5 min and a new calibration level of the Finapres was recorded before the servo was switched off again and another cycle of inflation/deflation took place. The technique used for the CO₂ reactivity test was based on that described by Bishop *et al* (1986). The baseline values of CBFV, ABP and EtCO₂ were recorded for an initial period of 5 min, while the subjects breathed normal air. This was followed by a 2 min recording with each subject breathing a mixture of 5% CO₂ in air, administered using a Douglas bag and elephant tubing leading to a one-way valve in the face mask. Finally, a 5 min recording of recovery data was taken with the subject once again breathing normal air. These recordings of spontaneous fluctuations of ABP and CBFV will be referred to as before, during and after the CO₂ test.

Table 1. Relation between K , D and T with ARI (adapted from Tiecks *et al* (1995)).

K	D	T	ARI
0.00	1.70	2.00	0
0.20	1.60	2.00	1
0.40	1.50	2.00	2
0.60	1.15	2.00	3
0.80	0.90	2.00	4
0.90	0.75	1.90	5
0.94	0.65	1.60	6
0.96	0.55	1.20	7
0.97	0.52	0.87	8
0.98	0.50	0.65	9

Data recorded on a magnetic tape were transferred to a computer and the maximum velocity envelope was extracted using an FFT algorithm with a 5 ms time window. The other signals were also sampled at 200 samples s^{-1} . All signals were low-pass filtered with an eighth order zero-phase Butterworth filter with a 20 Hz frequency cutoff. The beginning and end of each cardiac cycle were detected from the ECG, and the ABP and CBFV mean values were calculated for each cardiac cycle. The beat-to-beat time series were interpolated and resampled at five samples s^{-1} to obtain signals with a uniform time base.

2.2. Data analysis

The model proposed by Tiecks *et al* (1995) uses a second-order differential equation to predict the velocity signal $V(t)$ corresponding to a pressure change given by $P(t)$. Initially, the pressure change is normalized as

$$dP(t) = \frac{P(t)}{1 - CCP_r} \quad (1)$$

where CCP_r is a parameter introduced by Tiecks *et al* (1995) to represent the critical closing pressure as a fraction of the baseline pressure. The relative velocity change estimated by the model is given by

$$\hat{V}(t) = 1 + dP(t) - K \times x_2(t), \quad (2)$$

where K represents a gain parameter in the second-order equation and $x_2(t)$ is a state variable obtained from the following state equation system representing a second-order equation:

$$x_1(t) = x_1(t-1) + \frac{dP(t-1) - x_2(t-1)}{f \times T} \quad (3)$$

$$x_2(t) = x_2(t-1) + \frac{x_1(t-1) - 2 \times D \times x_2(t-1)}{f \times T}, \quad (4)$$

where f is the sampling frequency, T is the time constant and D is the damping factor. In the original proposal of Tiecks *et al* (1995), only ten combinations of the parameters K , D , T were considered, according to the values given in table 1, which also shows the corresponding value of ARI for each combination of these parameters.

The same procedure was used to fit the model to the data for spontaneous fluctuations and thigh cuff maneuvers. As adopted by Tiecks *et al* (1995), 30 s data windows were used

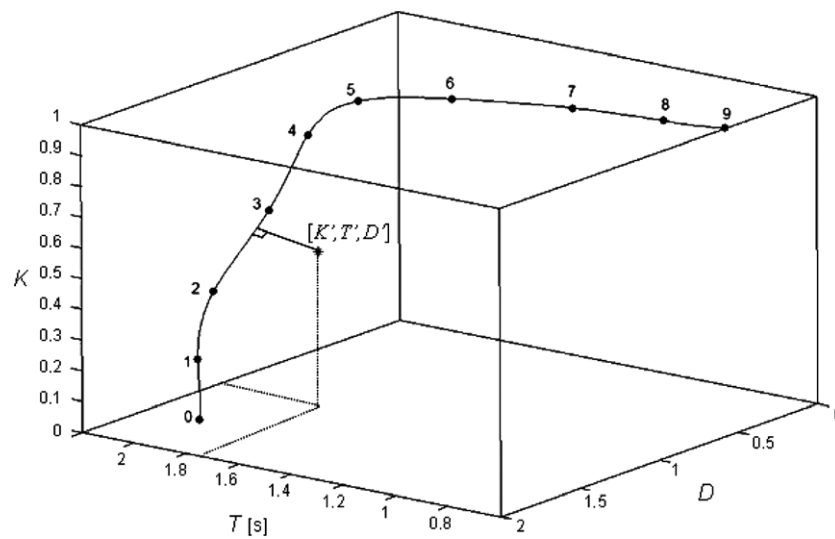


Figure 1. 3D representation of the K , D and T parameters of the original Aaslid–Tiecks model. The points on the curve represent the ten discrete values of the ARI. The solid line corresponds to a continuous index when K , D , T are interpolated.

to obtain estimates from thigh cuff maneuvers. For spontaneous fluctuations, 120 s segments of data were used. For each segment of data, the model generates ten velocity curves $\hat{V}(t)$, which are compared to the subject's actual velocity curve $V(t)$. The best fit is chosen based on the minimum quadratic error between $V(t)$ and $\hat{V}(t)$ or the maximum correlation coefficient between these two signals (Mahony *et al* 2000). From table 1, the corresponding values of K , D , T were then identified. Since $P(t)$ and $V(t)$ are normalized quantities in equations (1) and (2), the parameters K and D are adimensional whilst T is given in seconds.

Figure 1 gives a 3D representation of the relationship between the three model parameters (K , D , T) and the ten combinations selected by Tiecks *et al* (1995) to correspond to the ten different values of the ARI index. The figure also shows that a polynomial interpolation (spline) can be used to increase the number of possible states, by transforming the ten separate points into a continuous line in space. From the figure, it is clear that much of the total 'space' occupied by other combinations of $[K', D', T']$ is not used by the classical formulation of the model. By using other combinations of these parameters, it is possible to generate different model predictions $\hat{V}(t)$ and assess improvements in model fitting in relation to the results obtained with the combinations given in table 1.

A sensitivity analysis was performed to determine the smallest set of points to be considered when making the combinations, so as not to affect the accuracy factor considerably. It was determined that the parameter values did not change significantly when only 37 levels per parameter were adopted. When combining all possibilities of the three parameters, a total of 50 653 new combinations of K' , D' , T' could be used. For each segment of data, K' , D' , T' were estimated by least squares, or by maximizing the correlation coefficient between the model predicted values and data, using all the 50 653 possible combinations of these parameters.

Intra-subject variability of parameters for baseline recordings was assessed using the standard deviation (SD) of values obtained before, after 5% CO_2 and for the mean of the six thigh cuff maneuvers, as suggested by Bland and Altman (1986). To take into

Table 2. Mean \pm SD ($n = 16$) of physiological parameters during the four conditions studied.

Variable	Spontaneous fluctuations			
	Before CO ₂	5% CO ₂	After CO ₂	Thigh cuff
CBFV (cm s ⁻¹)	62.4 \pm 11.9	74.0 \pm 15.3	58.9 \pm 10.6	61.6 \pm 11.5
Mean BP (mmHg)	106.5 \pm 18.4	111.2 \pm 21.5	107.8 \pm 18.8	111.2 \pm 16.4
EtCO ₂ (mmHg)	42.6 \pm 3.1	48.4 \pm 2.2	41.4 \pm 2.1	–
Heart rate (bpm)	66.7 \pm 8.0	68.7 \pm 9.9	68.0 \pm 9.7	66.9 \pm 10.6

account differences in mean values between classical and unconstrained estimates, the SD was normalized by the mean and expressed as the per cent coefficient of variation (CV).

2.3. Statistical analysis

Paired Student's *t*-tests were used to test differences between parameters that satisfied the Shapiro–Wilks test of normality. For other parameters, differences were tested with the Wilcoxon paired test. A repeated measures MANOVA with between-effects was used to test the influence of the type of maneuvers (baseline, CO₂ challenge, or thigh cuff) and model fitting (constrained versus unconstrained) on values of *K*, *D*, *T*. A value of $p < 0.05$ was considered significant.

3. Results

Six thigh cuff maneuvers were performed in all 16 subjects. Seven maneuvers (in four subjects) were rejected due to artifacts in the CBFV recording, leaving a total of 89 thigh cuff maneuvers for analysis. Good quality baseline recordings during spontaneous fluctuations in ABP and CBFV were obtained in all 16 subjects. Table 2 contains the mean \pm SD values of physiological parameters before, during and after the CO₂ test, as well as for the six thigh cuff maneuvers.

3.1. Differences between parameters

The mean \pm SD of the estimated parameters are given in table 3, together with the values of ARI for the four different conditions considered. The correlation coefficient for the unconstrained parameters was always greater than the corresponding correlation for the original Aaslid–Tiecks model. The consistency of these differences led to highly significant ($p < 0.001$) results, as shown by the values in table 3, for both the thigh cuff maneuvers and spontaneous fluctuations. As an example, figure 2 depicts the improved fitting afforded by the unconstrained model for a thigh cuff maneuver in a representative subject.

The repeated measures MANOVA showed significant effects of measurement conditions on estimates of *T* ($p = 0.000\ 16$) and *K* ($p = 0.000\ 08$) (both classical and unconstrained), and significant effects of estimation method (classical versus unconstrained) only for *T* ($p = 0.000\ 006$) and *D* ($p = 0.000\ 13$). These effects can be better visualized by the plots in figure 3. For the 5% CO₂ breathing, there were significant differences between *D* and *D'* ($p = 0.007$) and *T* and *T'* ($p = 0.000\ 02$), but not between *K* and *K'*.

3.2. Intra-subject variability

Intra-subject CV was significantly smaller for *T* in comparison with *T'* (table 4). The coefficients of variation of both *K* and *K'* were significantly smaller than the one for the ARI.

Table 3. Distribution of parameters for classical ARI and unconstrained estimates of K , D , T , before, during and after 5% CO₂ and for the mean of six thigh cuff maneuvers. Values are mean \pm SD. See the text for MANOVA results.

Parameter	Spontaneous fluctuations							
	Before		5% CO ₂		After		Thigh cuff maneuvers	
	Classical	Unconstrained	Classical	Unconstrained	Classical	Unconstrained	Classical	Unconstrained
K	0.885 \pm 0.240	0.819 \pm 0.180	0.447 \pm 0.424	0.577 \pm 0.255	0.835 \pm 0.273	0.800 \pm 0.181	0.762 \pm 0.278	0.776 \pm 0.219
D	0.565 \pm 0.184	0.853 \pm 0.431	0.484 \pm 0.478	0.813 \pm 0.504	0.647 \pm 0.316	0.846 \pm 0.367	0.769 \pm 0.346	0.763 \pm 0.439
T	1.334 \pm 0.443	1.072 \pm 0.443	1.868 \pm 0.280	1.017 \pm 0.486	1.460 \pm 0.389	0.995 \pm 0.371	1.720 \pm 0.334	1.574 \pm 0.496
ARI	6.37 \pm 2.16	–	2.62 \pm 2.68	–	5.75 \pm 2.26	–	4.66 \pm 2.10	–
Correlation coefficient	0.548 \pm 0.153	0.598 \pm 0.151	0.642 \pm 0.160	0.689 \pm 0.163	0.582 \pm 0.123	0.619 \pm 0.124	0.777 \pm 0.162	0.821 \pm 0.149

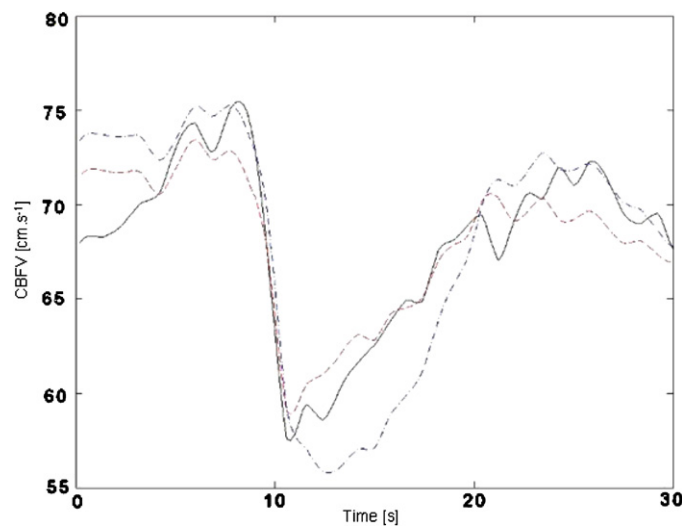


Figure 2. Representative thigh cuff maneuver in a 24 year old female subject. The recorded CBFV tracing (continuous line) is better fitted with the unconstrained parameters (dashed line), than with the original fixed parameter values adopted by the Aaslid–Tiecks model (dot-dashed line).

Table 4. Coefficients of variation (mean \pm SD) for baseline conditions (before, after and thigh cuff maneuvers) for parameters obtained with the classical model compared with unconstrained estimates.

Parameter	Coefficient of variation (%)	
	Classical	Unconstrained
K	20.1 \pm 24.3 ^a	14.2 \pm 7.0 ^a
D	23.0 \pm 22.6	26.9 \pm 14.0
T	17.9 \pm 12.8	30.7 \pm 12.5 ^b
ARI	27.8 \pm 24.5	–

^a $p < 0.005$ in comparison with ARI (Wilcoxon paired test).

^b $p < 0.05$ in comparison with the classical value.

3.3. Unconstrained parameter estimates for $ARI = 0$

Values of $ARI = 0$ should not be expected in healthy volunteers but a total of 15 occurrences were obtained for all the four measurement conditions studied. Figure 4 represents mean and SD values of K' , D' , T' against the corresponding values of classical ARI, for all the four conditions. These plots show that for higher values of ARI there is a good agreement between the classical and unconstrained parameter estimates. However, as ARI approaches zero, the corresponding values of K' , D' , T' tend to drift away from the corresponding values of K , D , T . For the 15 occurrences of $ARI = 0$, the mean \pm SD values of K' , D' , T' were respectively, 0.393 ± 0.138 , 0.500 ± 0.061 and 0.927 ± 0.440 s. There was a highly significant difference between these values and the corresponding classical values given in table 1 (Wilcoxon, $p < 0.007$).

Figure 5 sheds some light on the occurrence of values of classical $ARI = 0$ in healthy subjects. Using the mean values of K' , D' , T' given above for the 15 occurrences of $ARI = 0$, it is possible to estimate the velocity step response using equations (2)–(4). The beginning

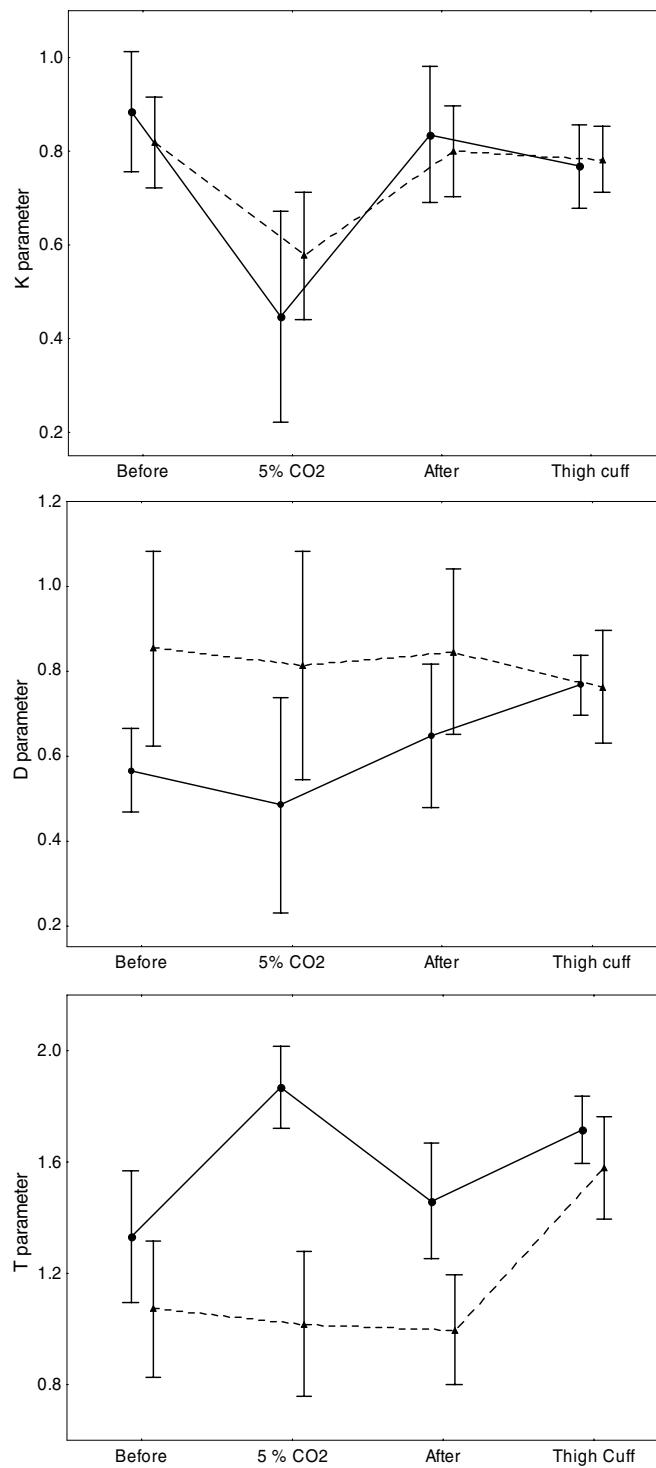


Figure 3. Mean \pm SD for parameters estimated according to the classical Aaslid-Tiecks model (continuous line), or with unconstrained values (dashed line), for four different measurement conditions. See the text for results of repeated measures MANOVA.

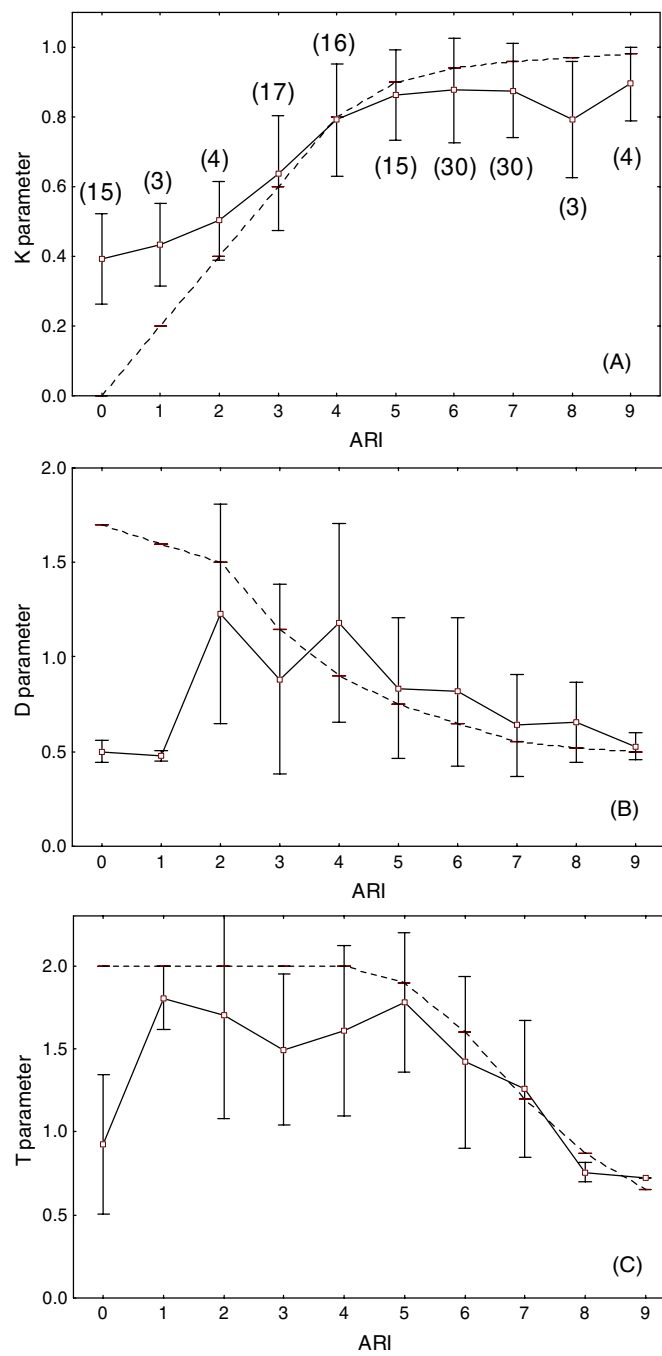


Figure 4. Distribution of mean \pm SD of the unconstrained parameters (continuous line), grouped according to ARI values and corresponding values of K , D , T parameters (dashed line) for the classical Aaslid-Tiecks model. The number of recordings contributing with ARI values in each category is indicated in brackets (A).

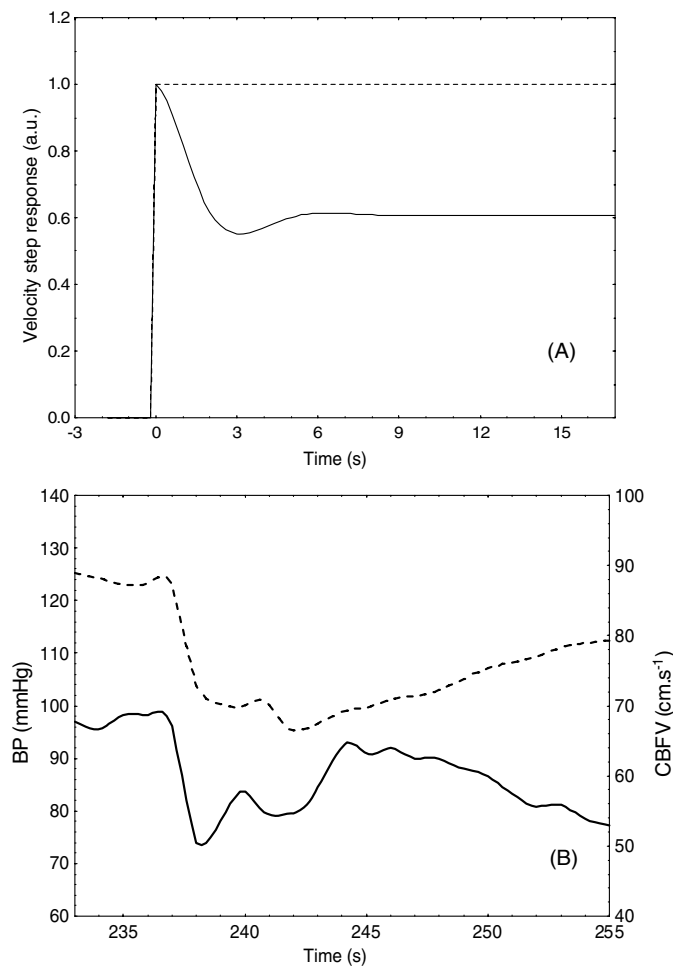


Figure 5. CBFV (continuous line) and BP (dashed line). (A) Aaslid–Tiecks model responses for mean values of K' , D' , T' corresponding to recordings with classical $ARI = 0$. (B) Thigh cuff responses from a 32 year old male subject classified as $ARI = 0$, but unconstrained parameters corresponding to $K' = 0.432$, $D' = 0.463$ and $T' = 1.935$.

of the response (figure 5(A)) suggests an active autoregulation, but the tail of the response does not reach the original baseline and this explains why the best-fit Aaslid–Tiecks model response applied over a 30 s window can lead to an $ARI = 0$. Figure 5(B) presents a thigh cuff response that was also classified as $ARI = 0$, but whose unconstrained parameters were close to the mean values used for the response in figure 5(A). Again, the beginning of the response suggests an active autoregulation but the CBFV drops again after 10 s and this probably led to a value of $ARI = 0$ when fitting the standard responses adopted by the classical Aaslid–Tiecks model.

4. Discussion

The main motivation for this study stemmed from the considerable variability reported for the ARI in both physiological and clinical studies (Mahony *et al* 2000, Panerai *et al* 2003, Simpson

et al 2004, Novak *et al* 2004, Hlatky *et al* 2006). By allowing the three main parameters of the second-order model proposed by Tiecks *et al* (1995) to assume values outside the rigid combination given in table 1, we have confirmed the hypothesis that better fitting between model and data can be obtained for all segments of data considered. On the other hand, other immediate advantages of this approach are less straightforward. In this regard, two important considerations are the sensitivity of model parameters to measurement reproducibility and also to the effects of arterial $p\text{CO}_2$ (PaCO_2).

Unconstrained parameters did not show significant improvements in intra-subject variability in comparison with classical values. Although the smaller CV of K' was not significantly different from that of K , both showed significantly smaller coefficients of variation in comparison with that of the ARI (table 4). Examining the different contributions of the three parameters for the generation of the standard velocity response curves that lead to the ARI index, it could be argued that K has a dominant influence, as seen from the values in table 1 and the plots in figure 4. Consequently, despite the unconstrained parameters not showing better reproducibility, the fact that the minimum numerical value was observed for the gain (K') is of some importance, and can lead to an improved index of dynamic autoregulation as discussed later.

The sensitivity of the parameters to reflect changes in dynamic autoregulation induced by breathing 5% CO_2 is also relevant. The results in table 3 and figure 3 indicate that T' is less sensitive to the effects of CO_2 than T , but there were no significant differences between K and K' . Considering that the time constant T remains approximately constant for values of ARI < 6 (table 1 and figure 4(C)), these results suggest that, overall, there are no major differences in sensitivity to PaCO_2 between the unconstrained and classical estimates of K , D , T . However, as discussed below, there are other important considerations involving the stability of ARI estimates, and consequently of the corresponding values of K , D , T .

In previous studies, the stability and variability of the ARI have been compromised by the occurrence of values of ARI = 0 in healthy subjects (Carey *et al* 2000, Mahony *et al* 2000, Panerai *et al* 2003). According to the values in table 1, if ARI = 0, then $K = 0.0$, $D = 1.70$ and $T = 2.0$. As shown in figure 4, for the occurrences of ARI = 0, the corresponding unconstrained parameters showed very different mean values, corresponding to a velocity step response that is different from any of the template curves adopted by the Aaslid–Tiecks model (figure 5(A)). This result has several important implications. First, the fact that K' never reached values close to zero suggests that the unconstrained parameters are more robust against physiological variability as manifested in different temporal patterns of the velocity step response. Second, the departure of K' , D' , T' from K , D , T for smaller values of ARI (figure 4) leads to the speculation that the unidimensional concept of the ARI might not be entirely applicable as a measure of dynamic cerebral autoregulation. As shown by the responses in figure 5, the velocity response curves adopted by the Aaslid–Tiecks model (Tiecks *et al* 1995) cannot represent velocity responses that seem to combine both active and poor autoregulation. Similar responses have been observed in many other studies (Carey *et al* 2000, Panerai *et al* 1999a, 2001, 2004, Sato *et al* 2001). Whether these temporal patterns suggesting mixed responses are reflecting different dynamic behavior of separate mechanisms involved in the regulation of CBF (e.g., myogenic versus metabolic) would be an exciting line of investigation for the future.

Despite the lack of overwhelming evidence favoring the unconstrained parameters in comparison with classical values, when different aspects of the study are put together, it is possible to make the case for K' replacing ARI as a single index of dynamic autoregulation. First of all, K' showed more stable behavior compared with the ARI, by not having the same ‘crashes’ to zero values as observed in 15 different recordings. Second, K' maintained the

same sensitivity to the effects of changes in PaCO_2 as K . Although the values of ARI during the CO_2 test (table 3) suggest that it can be much more sensitive to PaCO_2 than either K or K' , this is misleading because it includes values of $\text{ARI} = 0$ in 7 of the 16 subjects studied. Dynamic autoregulation is expected to be reduced due to 5% CO_2 breathing (Aaslid *et al* 1989, Panerai *et al* 1999b), but not entirely abolished in healthy subjects as it would be suggested by the values of $\text{ARI} = 0$. Finally, the significantly smaller intra-subject variability of K' during baseline recordings, in comparison with ARI (table 4), would also be an important advantage. Future studies are needed to test this proposal, by comparing K' with the classical ARI under a wide range of physiological and clinical conditions. Although K or K' can be seen as reflecting the steady-state response of the Tiecks model, in the context of steady responses, equations (1)–(4) show that the values of $K = K' = 0$ would lead to an absence of autoregulation, that is $\Delta V(t \rightarrow \infty) = \Delta P(t \rightarrow \infty)$, whilst $K = K' = 1$ would represent perfect autoregulation with $\Delta V(t \rightarrow \infty) = 0$.

A major limitation of this study is the absence of patients with cerebrovascular conditions. The 5% CO_2 test was adopted as a surrogate of cerebral autoregulation impairment, but it cannot reflect the extent and different pathways by which cerebral autoregulation can be damaged in patients with different pathologies, for example, carotid artery disease, stroke or severe head injury. Limitations related to measurement techniques also apply, but are less likely to affect the conclusions of the study, since comparative analyses were performed intra-recordings. Nevertheless, increased variability, or even, instability of the ARI, could also be due to the non-invasive methods of measurement adopted by most studies of cerebral autoregulation. Ultrasound Doppler measurements of CBFV in the MCA could be distorted by changes in arterial diameter, thus altering the relationship between CBFV and true CBF. Hitherto, significant changes in MCA diameter have not been reported, even in the presence of changes in ABP and PaCO_2 much above what was observed in this study (Giller *et al* 1993, Newell *et al* 1994, Serrador *et al* 2000). Non-invasive measurements of ABP with the Finapres could also have led to a mismatch between finger and central ABP and, hence, to changes in the ARI value (Birch and Morris 2003, Panerai *et al* 2006). Nevertheless, a recent study has found that dCA measurements with the Finapres showed excellent agreement with corresponding estimates derived from intra-aortic recordings, including the ARI (Sammons *et al* 2007). Additional studies should take these factors into account, possibly comparing the inherent variability of ARI with other measures of dCA, such as transfer function analysis parameters. Finally, it could be argued that replacing the ARI index by K' or another index, but still maintaining an unidimensional scale, leads to sub-optimal assessment of dCA. Unfortunately, it is still not clear how many different dimensions are needed to fully reflect the phenomenon of dynamic cerebral autoregulation and its alterations under different clinical conditions.

5. Conclusions

Allowing the main parameters of the second-order differential equation model proposed by Tiecks *et al* (1995) to take a wider range of values can lead to improvements in model accuracy and parameter stability. Although unconstrained parameters are significantly different from the classical values used by the Aaslid–Tiecks model, they can still be sensitive to different conditions, such as changes in PaCO_2 , and can display reduced intra-subject variability in comparison with the classical ARI. Future studies are necessary to confirm these findings in larger and more diverse populations and also to test the properties of the unconstrained parameters under different clinical conditions.

Acknowledgments

This work was supported by a grant from the Comisión Nacional de Investigación Científica y Tecnológica—Chile (CONICYT, Projects 1050082 and 7060067). The authors would like to thank Professor David H Evans and Dr Lingke Fan for the development of the Doppler analyser software and Mr. Felipe Bello for his help with the preparation of the manuscript.

References

- Aaslid R, Lindegaard K F, Sorteberg W and Normes H 1989 Cerebral autoregulation dynamics in humans *Stroke* **20** 45–52
- Birch A A and Morris S L 2003 Do the Finapres and Colin radial artery tonometer measure the same blood pressure changes following deflation of thigh cuffs? *Physiol. Meas.* **24** 653–60
- Bishop C C R, Powell S, Insall M and Rutt N L 1986 Effect of internal carotid artery occlusion on middle cerebral artery blood flow at rest and in response to hypercapnia *Lancet* **1** 710–12
- Bland J M and Altman D G 1986 Statistical methods to assess agreement between two methods of clinical measurement *Lancet* **1** 307–10
- Carey B J, Eames P J, Panerai R B and Potter J F 2000 Dynamic cerebral autoregulation is unaffected by aging *Stroke* **31** 2895–900
- Dawson S L, Blake M J, Panerai R B and Potter J F 2000 Dynamic but not static cerebral autoregulation is impaired in acute ischaemic stroke *Cerebrovasc. Dis.* **10** 126–32
- Doering T J, Aaslid R, Steuernagel B, Brix J, Niederstadt C, Breull A B, Schneider B and Fischer G C 1999 Cerebral autoregulation during whole-body hypothermia and hyperthermia stimulus *Am. J. Phys. Med. Rehabil.* **78** 33–8
- Eames P J, Blake M J, Panerai R B and Potter J F 2003 Cerebral autoregulation indices are unimpaired by hypertension in middle aged and older people *Am. J. Hypert.* **16** 746–53
- Giller C A 1990 The frequency-dependent behavior of cerebral autoregulation *Neurosurgery* **27** 362–8
- Giller C A, Bowman G, Dyer H, Mootz L and Krippner W 1993 Cerebral arterial diameters during changes in blood pressure and carbon dioxide during craniotomy *Neurosurgery* **32** 737–42
- Hlatky R, Valadka A B and Robertson C S 2006 Analysis of dynamic autoregulation assessed by the cuff deflation method *Neurocrit. Care* **4** 127–32
- Junger E C, Newell D W, Grant G A, Avellino A M, Ghatan S, Douville C M, Lam A M, Aaslid R and Winn H R 1997 Cerebral autoregulation following minor head injury *J. Neurosurg.* **86** 425–32
- Leftheriotis G, Dupuis J M and Victor J 2000 Cerebral hemodynamics in carotid sinus syndrome and atrioventricular block *Am. J. Cardiol.* **86** 504–8
- Mahony P, Panerai R B, Deverson S T, Hayes P D and Evans D H 2000 Assessment of the thigh cuff technique for measurement of dynamic cerebral autoregulation *Stroke* **31** 477–80
- Newell D W, Aaslid R, Lam A M, Mayberg T S and Winn H R 1994 Comparison of flow and velocity during dynamic autoregulation testing in humans *Stroke* **25** 793–7
- Newell D W, Weber J P, Watson R, Aaslid R and Winn H R 1996 Effect of transient moderate hyperventilation on dynamic cerebral autoregulation after severe head injury *Neurosurgery* **39** 35–44
- Novak V, Yang A C C, Lepicovsky L, Goldberger A L, Lipsitz L A and Peng C K 2004 Multimodal pressure-flow method to assess dynamics of cerebral autoregulation in stroke and hypertension *Bio. Med. Eng. OnLine* **3** 39
- Panerai R B, Dawson S L and Potter J F 1999a Linear and nonlinear analysis of human dynamic cerebral autoregulation *Am. J. Physiol. Heart Circ. Physiol.* **277** H1089–99
- Panerai R B, Dawson S L, Eames P J and Potter J F 2001 Cerebral blood flow velocity response to induced and spontaneous sudden changes in arterial blood pressure *Am. J. Physiol. Heart Circ. Physiol.* **280** H2162–74
- Panerai R B, Deverson S T, Mahony P, Hayes P and Evans D H 1999b Effect of CO₂ on dynamic cerebral autoregulation measurement *Physiol. Meas.* **20** 265–75
- Panerai R B, Eames P J and Potter J F 2003 Variability of time-domain indices of dynamic cerebral autoregulation *Physiol. Meas.* **24** 367–81
- Panerai R B, Kelsall A R, Rennie J M and Evans D H 1995 Cerebral autoregulation dynamics in premature newborns *Stroke* **26** 74–80
- Panerai R B, Kerins V, Fan L, Yeoman P M, Hope T and Evans D H 2004 Association between dynamic cerebral autoregulation and mortality in severe head injury *Brit. J. Neurosurg.* **18** 471–9
- Panerai R B *et al* 2006 Cerebral critical closing pressure estimation from Finapres and arterial blood pressure measurements in the aorta *Physiol. Meas.* **27** 1387–402

- Paulson O B, Strandgaard S and Edvinson L 1990 Cerebral autoregulation *Cerebrovasc. Brain Metab. Rev.* **2** 161–92
- Sammons E L *et al* 2007 Differences in Finapres and direct intra-arterial derived measures of dynamic cerebral autoregulation *J. Appl. Physiol.* **103** 369–75
- Sato J, Tachibana M, Numata T, Nishino T and Konn A 2001 Differences in the dynamic cerebrovascular response between stepwise up tilt and down tilt in humans *Am. J. Physiol. Heart Circ. Physiol.* **281** H774–83
- Serrador J M, Picot P A, Rutt B K, Shoemaker J K and Bondar R L 2000 MRI measures of middle cerebral artery diameter in conscious humans during simulated orthostasis *Stroke* **31** 1672–8
- Simpson D M, Panerai R B, Ramos E G, Lopes A J, Marinatto M N, Nadal J and Evans D H 2004 Assessing blood flow control through a bootstrap method *IEEE Trans. Biomed. Eng.* **51** 1284–6
- Steiger H J, Aaslid R, Stoos R and Seiler R W 1994 Transcranial Doppler monitoring in head injury: relations between type of injury, flow velocities, vasoreactivity, and outcome *Neurosurgery* **34** 79–86
- Steinmeier R *et al* 1996 Slow rhythmic oscillations of blood pressure, intracranial pressure, microcirculation, and cerebral oxygenation: dynamic interrelation and time course in humans *Stroke* **27** 2236–43
- Tiecks F, Lam A M, Aaslid R and Newell D W 1995 Comparison of static and dynamic cerebral autoregulation measurements *Stroke* **26** 1014–9
- Vavilala M S, Newell D W, Junger E, Douville C M, Aaslid R, Rivara F P and Lam A M 2002 Dynamic cerebral autoregulation measurements *Stroke* **26** 397–7
- White R P and Markus H S 1997 Impaired dynamic cerebral autoregulation in carotid artery stenosis *Stroke* **28** 1340–4